Axl mediates ZIKA virus entry in human glial cells and modulates innate immune responses

Laurent Meertens, Athena Labeau, Ophélie Dejarnac, Sara Cipriani, Laura Sinigaglia, Lucie Bonnet-Madin, Tifenn Le Charpentier, Mohamed Lamine Hafirassou, Alessia Zamborlini, Van-Mai Cao-Lormeau, et al.

Report

Cell Reports

Axl Mediates ZIKA Virus Entry in Human Glial Cells and Modulates Innate Immune Responses

Graphical Abstract

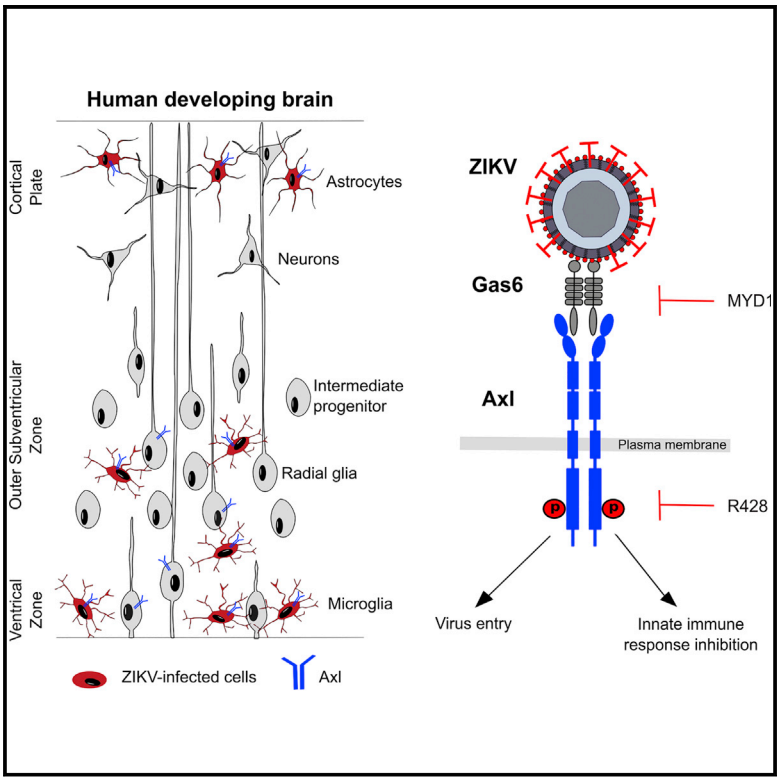

Authors

Laurent Meertens, Athena Labeau, Ophelie Dejarnac, ..., Pierre Gressens, Olivier Schwartz, Ali Amara

Correspondence

laurent.meertens@inserm.fr (L.M.), ali.amara@inserm.fr (A.A.)

In Brief

ZIKA virus (ZIKV) is responsible for congenital microcephaly. Meertens et al. show that the Axl receptor is expressed in microglia and astrocytes in the human developing brain. They also highlight the dual role of Axl during infection, which promotes viral entry and dampens innate immune responses in glial cells.

Highlights

- Microglial cells and astrocytes in the human developing brain express Axl
- Axl binds ZIKV through Gas6 bridging and promotes ZIKV infection of glial cells
- ZIKV-Gas6 complexes activate Axl during viral entry to dampen innate immunity
- The Axl decoy receptor MYD1 and the Axl kinase inhibitor R428 inhibit ZIKV infection

Meertens et al., 2017, Cell Reports *18*, 324–333
January 10, 2017
http://dx.doi.org/10.1016/j.celrep.2016.12.045

OPEN ACCESS
CellPress

Cell Reports
Report

Axl Mediates ZIKA Virus Entry in Human Glial Cells and Modulates Innate Immune Responses

Laurent Meertens,[1,2,3,*] Athena Labeau,[1,2,3] Ophelie Dejarnac,[1,2,3] Sara Cipriani,[4] Laura Sinigaglia,[5] Lucie Bonnet-Madin,[1,2,3] Tifenn Le Charpentier,[4] Mohamed Lamine Hafirassou,[1,2,3] Alessia Zamborlini,[1,2,3,6] Van-Mai Cao-Lormeau,[7] Muriel Coulpier,[8] Dorothée Missé,[9] Nolwenn Jouvenet,[5] Ray Tabibiazar,[10] Pierre Gressens,[4] Olivier Schwartz,[11] and Ali Amara[1,2,3,12,*]

[1]INSERM U944, CNRS 7212 Laboratoire de Pathologie et Virologie Moléculaire, Hôpital Saint-Louis, 1 avenue Claude Vellefaux, 75010 Paris, France
[2]Institut Universitaire d'Hématologie, Hôpital Saint-Louis, 1 avenue Claude Vellefaux, 75010 Paris, France
[3]University Paris Diderot, Sorbonne Paris Cité, Hôpital St. Louis, 1 avenue Claude Vellefaux, 75475 Paris Cedex 10, France
[4]PROTECT, INSERM, Université Paris Diderot, Sorbonne Paris Cité, 75019 Paris, France
[5]UMR CNRS 3569, Viral Genomics and Vaccination Unit, Pasteur Institute, 75724 Paris, France
[6]Laboratoire PVM, Conservatoire des Arts et Metiers, 292 Rue Saint-Martin, 75003 Paris, France
[7]Institut Louis Malardé, Papeete, Tahiti, French Polynesia
[8]ANSES, Université Paris-Est, Ecole Nationale Vétérinaire d'Alfort, UMR Virologie, 94700 Maisons-Alfort, France
[9]Laboratoire MIVEGEC, UMR 224 IRD/CNRS, 34394 Montpellier, France
[10]Ruga Corporation, Two Houston Center, 909 Fannin St., #2000, Houston, TX 77010-1018, USA
[11]Unité Virus et Immunité, Institut Pasteur, 28 rue du Dr. Roux, 75724 Paris, France
[12]Lead Contact
*Correspondence: laurent.meertens@inserm.fr (L.M.), ali.amara@inserm.fr (A.A.)
http://dx.doi.org/10.1016/j.celrep.2016.12.045

SUMMARY

ZIKA virus (ZIKV) is an emerging pathogen responsible for neurological disorders and congenital microcephaly. However, the molecular basis for ZIKV neurotropism remains poorly understood. Here, we show that Axl is expressed in human microglia and astrocytes in the developing brain and that it mediates ZIKV infection of glial cells. Axl-mediated ZIKV entry requires the Axl ligand Gas6, which bridges ZIKV particles to glial cells. Following binding, ZIKV is internalized through clathrin-mediated endocytosis and traffics to Rab5+ endosomes to establish productive infection. During entry, the ZIKV/Gas6 complex activates Axl kinase activity, which downmodulates interferon signaling and facilitates infection. ZIKV infection of human glial cells is inhibited by MYD1, an engineered Axl decoy receptor, and by the Axl kinase inhibitor R428. Our results highlight the dual role of Axl during ZIKV infection of glial cells: promoting viral entry and modulating innate immune responses. Therefore, inhibiting Axl function may represent a potential target for future antiviral therapies.

INTRODUCTION

ZIKA virus (ZIKV) is a mosquito-borne flavivirus originally isolated from a sentinel monkey in the Zika Forest of Uganda (Dick et al., 1952). Recent ZIKV outbreaks in French Polynesia and in Brazil, which expanded rapidly throughout South and Central America, have raised concerns about the pathogenicity of ZIKV. Infection by ZIKV has been linked to several neurological disorders, including Guillain-Barré syndrome, meningoencephalitis, and myelitis (White et al., 2016). Infection of pregnant women is associated with fetal abnormalities, congenital microcephaly, and abortion (Brasil et al., 2016; Mlakar et al., 2016), with evidence of ZIKV detected in fetal brain tissues or amniotic fluid (Calvet et al., 2016; Mlakar et al., 2016). Recent studies using murine models of infection provided direct evidence for ZIKV vertical transmission, leading to fetal abnormalities and brain development defects in the offspring (Li et al., 2016a; Miner et al., 2016a; Wu et al., 2016). In the developing fetal brain, ZIKV targets neural progenitor cells, alters cell division, and induces cell death, hampering brain development (Li et al., 2016a; Wu et al., 2016).

Identifying ZIKV entry factors represents a major challenge in the understanding of ZIKV tropism and pathogenesis. We recently showed that expression of several known flavivirus entry factors, including Axl, confers sensitivity to ZIKV in otherwise poorly susceptible cells (Hamel et al., 2015). Neutralizing antibodies or small interfering RNA targeting Axl drastically reduced ZIKV infection in primary dermal fibroblasts (Hamel et al., 2015), supporting a crucial role for Axl in ZIKV biology. In agreement with this model, RNA sequencing (RNA-seq) and immunochemistry studies confirmed that human neural progenitors cells, which support productive ZIKV infection both in vitro and in vivo (Li et al., 2016a; Tang et al., 2016; Wu et al., 2016), express Axl (Nowakowski et al., 2016). Axl mRNA is present in other brain cells, including radial glial cells, astrocytes, and microglial cells (Nowakowski et al., 2016). However, the effective contribution of Axl in ZIKV infection of these cells remains to be determined.

Axl belongs to the Tyro3 Axl Mer (TAM) family, a group of tyrosine kinase receptors involved in the clearance of apoptotic cells and regulation of innate immunity (Lemke and Rothlin, 2008;

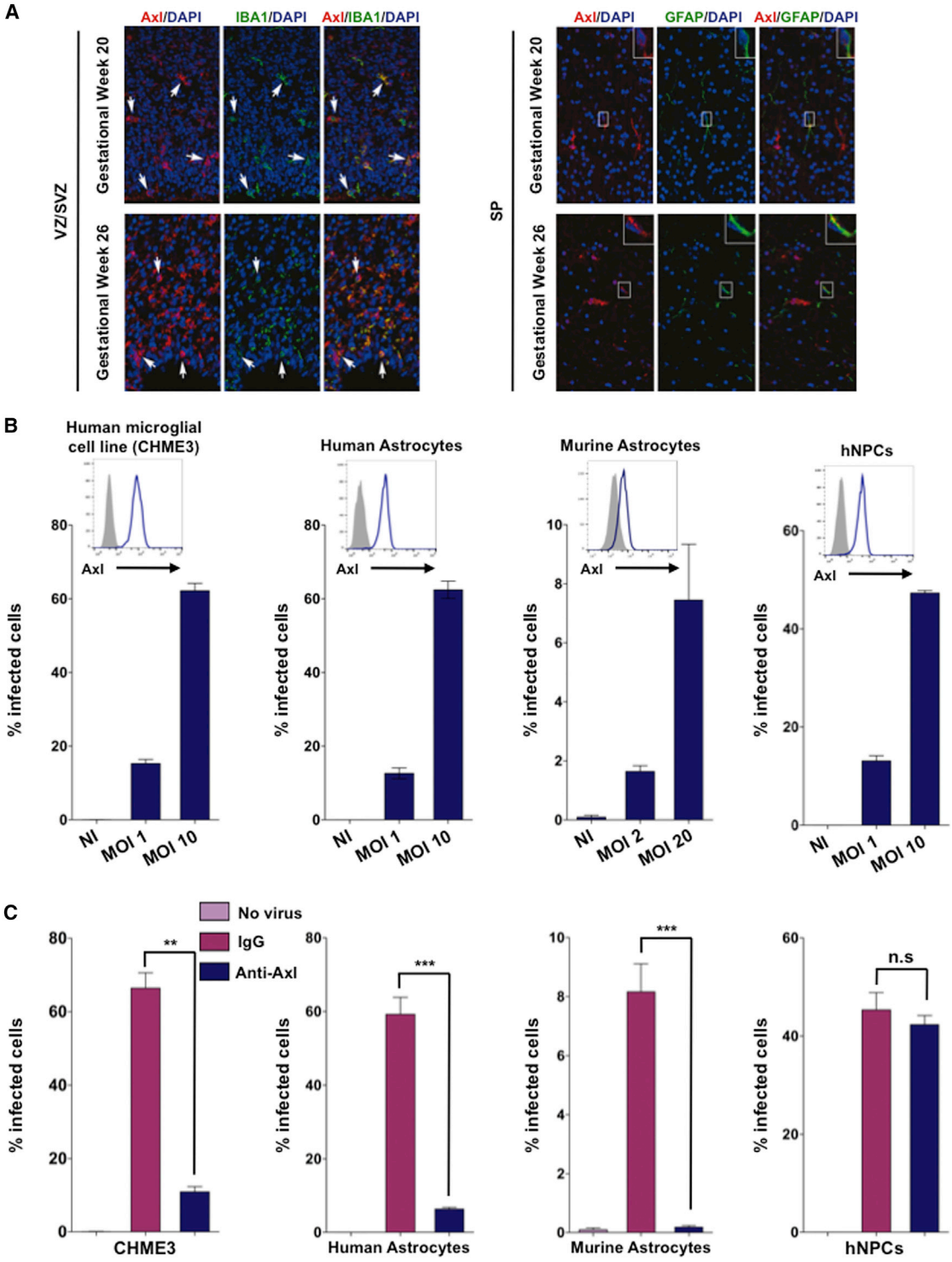

Figure 1. Essential Role of Axl in ZIKV Infection of Human Glial Cells but Not hNPCs

(A) Axl immunostaining in the human developing cerebral cortex. Axl expression is observed in microglia (IBA1+) (left) and radial glia, and astrocytes (GFAP+) (right). High magnifications of Axl/GFAP cells are shown in the respective picture inset. White arrows indicate strong signal colocalization.

(B) The human microglial cell line (CHME3), human and murine primary astrocytes, and hNPCs were challenged with ZIKV at the indicated MOI. Insets display cell surface expression of Axl.

(legend continued on next page)

Rothlin et al., 2007). We have previously identified Axl as an entry factor for dengue virus (DENV) (Meertens et al., 2012). DENV binds indirectly to Axl through Gas6, the natural ligand of Axl, which recognizes phosphatidylserine (PS) exposed at the surface of the viral envelope and bridges the viral particle to the Axl receptor. This mechanism of viral entry, based on PS exposure, has been extended to other viruses and is termed viral apoptotic mimicry (Amara and Mercer, 2015). In addition to its role in virus entry, Axl also mediates signaling through its tyrosine kinase domain to dampen type I interferon (IFN) signaling and facilitate infection (Bhattacharyya et al., 2013; Meertens et al., 2012).

We report here that Axl is a crucial receptor for ZIKV infection of human glial cells (astrocytes and microglia). We also describe the dual role played by Axl, promoting viral entry and modulating innate immune responses. We identify two inhibitors, the Axl decoy receptor MYD1 and the Axl kinase inhibitor R428, that efficiently inhibit ZIKV infection. Altogether, our study provides important insights into the molecular interactions occurring upon ZIKV entry into human glial cells.

RESULTS AND DISCUSSION

Axl Is Expressed in Glial Cells in the Developing Brain and mediates ZIKV infection

Single-cell mRNA sequencing studies have shown that the "ZIKV entry receptor *Axl* is enriched in radial glia, microglia, and astrocytes" in the developing human cortex (Nowakowski et al., 2016). Here we assessed whether the Axl protein could be detected in microglia and astrocytes during human cortical development. At 20 gestational weeks (GWs), Axl was strongly and widely expressed in microglia (Iba1+ cells) that mainly localized in the ventricular zone (VZ) and subventricular zone (SVZ) (Figure 1A). Closer examination revealed that Axl labeling could be observed in GFAP+ cells, such as radial glial progenitor cells along the ventricle border and in a few differentiating subplate astrocytes (Figure 1A). At a more advanced stage of development (26 GWs), microglial cells became denser in the VZ/SVZ, remaining strongly immunoreactive to Axl antibodies (Abs) (Figure 1A). In parallel, Axl was occasionally observed in residual GFAP+ radial glial cells of the VZ and also remained detectable in maturing astrocytes (Figure 1A). Based on this expression pattern, we postulated that astrocytes and microglial cells might be major ZIKV targets. Therefore, we investigated the susceptibility of the CHME3 microglial cell line, primary human and murine astrocytes, and human neural progenitor cells (hNPCs) to ZIKV infection. In agreement with the expression profile of Axl in the human fetal brain and data from the literature (Ji et al., 2013; Nowakowski et al., 2016), all of these cells expressed high levels of Axl (Figure 1B), but not on murine microglial cells, as described previously (Fourgeaud et al., 2016; Ji et al., 2013; Figure 1B; Figure S1A). We challenged these cells with the African ZIKV strain HD78788 (ZIKVHD78) at MOIs of 1 and 10. The percentage of infected cells was quantified 24 hr later by flow cytometry using the pan-flavivirus anti-E protein Ab 4G2. CHME3 cells, human and murine astrocytes, and hNPCs were productively infected by ZIKV (Figure 1B; Figure S1B), whereas murine microglial cells were resistant to ZIKV and other flaviviruses (Figure S1A). ZIKV infection of human and murine primary astrocytes and CHME3 cells was abrogated by an anti-Axl polyclonal Ab (pAb) but not a control pAb (Figure 1C), or by silencing Axl expression by small interfering RNA (siRNA) (Figure S1C). In contrast, the anti-Axl Ab did not significantly affect ZIKV infection of hNPCs (Figure 1C, right), suggesting the existence of additional ZIKV entry receptors in these cells. We then asked whether the related flavivirus DENV, which also exploits Axl as an entry molecule (Meertens et al., 2012), has the same tropism as ZIKV in neuronal cells. DENV productively infected CHME3, murine astrocytes and hNPCs in an Axl-dependent manner (Figures S1D and S1E), which is consistent with neurological complications and neuroinvasion reported in numerous cases of DENV (Carod-Artal et al., 2013). Our data reveal common entry pathways for ZIKV and DENV in brain cells, although additional mechanisms such as the ability to cross the blood-brain barrier (BBB), access to brain cells, and/or virus-associated inflammation may explain the variety and extent of neuropathological manifestations observed with different flaviviruses.

The Axl Decoy Receptor MYD1 Sequesters Gas6 and Inhibits ZIKV Infection

To investigate whether Axl-mediated ZIKV infection is dependent on the TAM ligands Gas6 and Protein S (ProS) (Lemke and Rothlin, 2008), CHME3 cells were infected with ZIKVHD78 in the absence of fetal calf serum (FCS), which naturally contains TAM ligands (Fernández-Fernández et al., 2008). ZIKV infection of CHME3 was dramatically reduced under serum-free conditions (Figure 2A). Addition of Gas6 restored ZIKV infection at a level comparable with control cells. Thus, Axl-mediated ZIKV-infection is dependent on Gas6. Our results support a tripartite model in which Gas6 binds to PS at the surface of ZIKV and bridges virions to the Axl receptor. MYD1 is an engineered Axl decoy receptor that displays a high affinity for human Gas6 and blocks the ligand-receptor interaction through complete neutralization of Gas6 (Kariolis et al., 2014). MYD1 inhibited ZIKV in a dose-dependent manner (Figure 2B) but displayed negligible effects on herpes simplex virus type 1 (HSV-1), a neurotropic virus that infects cells independently of Axl (Meertens et al., 2012). In addition, MYD1 inhibited ZIKV binding to CHME3 cells (Figure 2C). We observed similar results in HeLa cells stably expressing Axl (HeLa-Axl) (Figures S1A and S1B). Infection of primary astrocytes (Figure 2D) or CHME3 cells (Figure S1C) was also inhibited by MYD1 in the presence of FCS. Because MYD1 has negligible binding to ProS (Kariolis et al., 2014), these results suggest that Gas6 is the primary driver for ZIKV infection in glial cells. To test this hypothesis, we incubated primary astrocytes and CHME3 with an anti-Gas6 pAb before challenge with ZIKV. The anti-Gas6 pAb, but not the control immunoglobulin (Ig), inhibited ZIKV infection (Figure 2E;

(C) CHME3, human and murine primary astrocytes, and hNPCs were pre-incubated for 30 min with neutralizing goat anti-Axl or goat IgG prior to infection with ZIKV (MOI 10).

(B and C) Infection was assessed 24 or 48 hpi (murine astrocytes) by flow cytometry. Data shown are means ± SD of three independent experiments. Significance was calculated using a two-sample Student's t test (n.s., not significant; **$p < 0.001$; ***$p < 0.0001$).

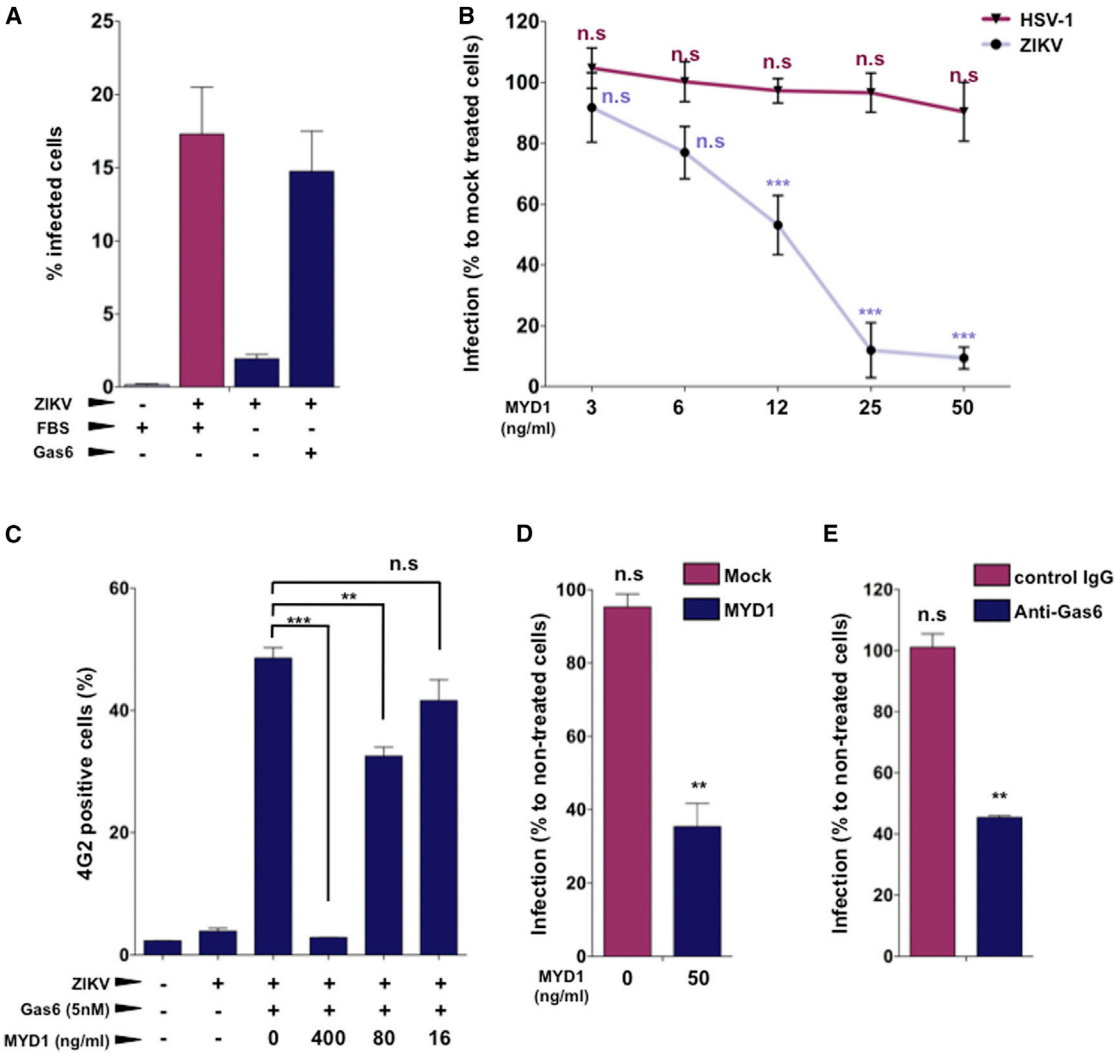

Figure 2. The MYD1 Decoy Receptor Inhibits ZIKV Infection

(A) Serum-starved CHME3 cells were challenged with ZIKV in DMEM alone or containing rhGas6 (1 nM). Data shown are means ± SD and are representative of three independent experiments.

(B) Serum-starved CHME3 cells were challenged with ZIKV (MOI 5) and HSV-1 (MOI 0.5) particles incubated prior to infection with rhGas6 (1 nM) in combination with the indicated concentration of MYD1 or vehicle (mock).

(C) CHME3 cells were incubated with ZIKV (MOI 100) with or without rhGas6 (5 nM) in the presence of the indicated concentration of MYD1 for 1 hr at 4°C. Cell surface-bound particles were stained with the 4G2 mAb and detected by flow cytometry. Data shown are means ± SD and are representative of two independent experiments performed in duplicate.

(D) Astrocytes were challenged with ZIKV (MOI 5) incubated prior to infection with the indicated concentration of MYD1 or vehicle (mock).

(E) Astrocytes were incubated with polyclonal goat anti-hGas6 or a control IgG and infected with ZIKV (MOI 10) in the continuous presence of the antibodies. Infection was assessed 24 hpi by flow cytometry using the respective anti-viral protein antibodies.

(B, D, and E) The data shown are means ± SD of two or three independent experiments. Significance was calculated using a one-way ANOVA statistical test with a Dunnett's multiple comparisons test (B and C) or a two-sample Student's t test (D and E). *$p < 0.05$, **$p < 0.001$, ***$p < 0.0001$).

Figure S1D). Altogether, our results suggest that the decoy Axl receptor MYD1 blocks ZIKV infection by sequestering Gas6 and preventing virus binding to Axl.

ZIKV Enters Axl-Expressing Cells by Clathrin-Mediated Endocytosis and Traffics through Early Endosomes

To further investigate the mechanisms of ZIKV entry, we used the clustered regularly interspaced short palindromic repeats (CRISPR)-CRISPR associated protein 9 (Cas9) technology to stably knock down Axl expression in CHME3 cells (Axl^{KO}) (Figure 3A). Axl^{KO} and parental CHME3 cells were then challenged with ZIKVHD78 or the ZIKV strain H/PF/2013, a clinical strain isolated from a patient in French Polynesia and closely related to the epidemic strains from South and Central America (Calvet et al., 2016). Infection with both the ZIKVHD78 and ZIKV H/PF/2013 strains was abrogated in Axl^{KO} cells (Figure 3B), whereas

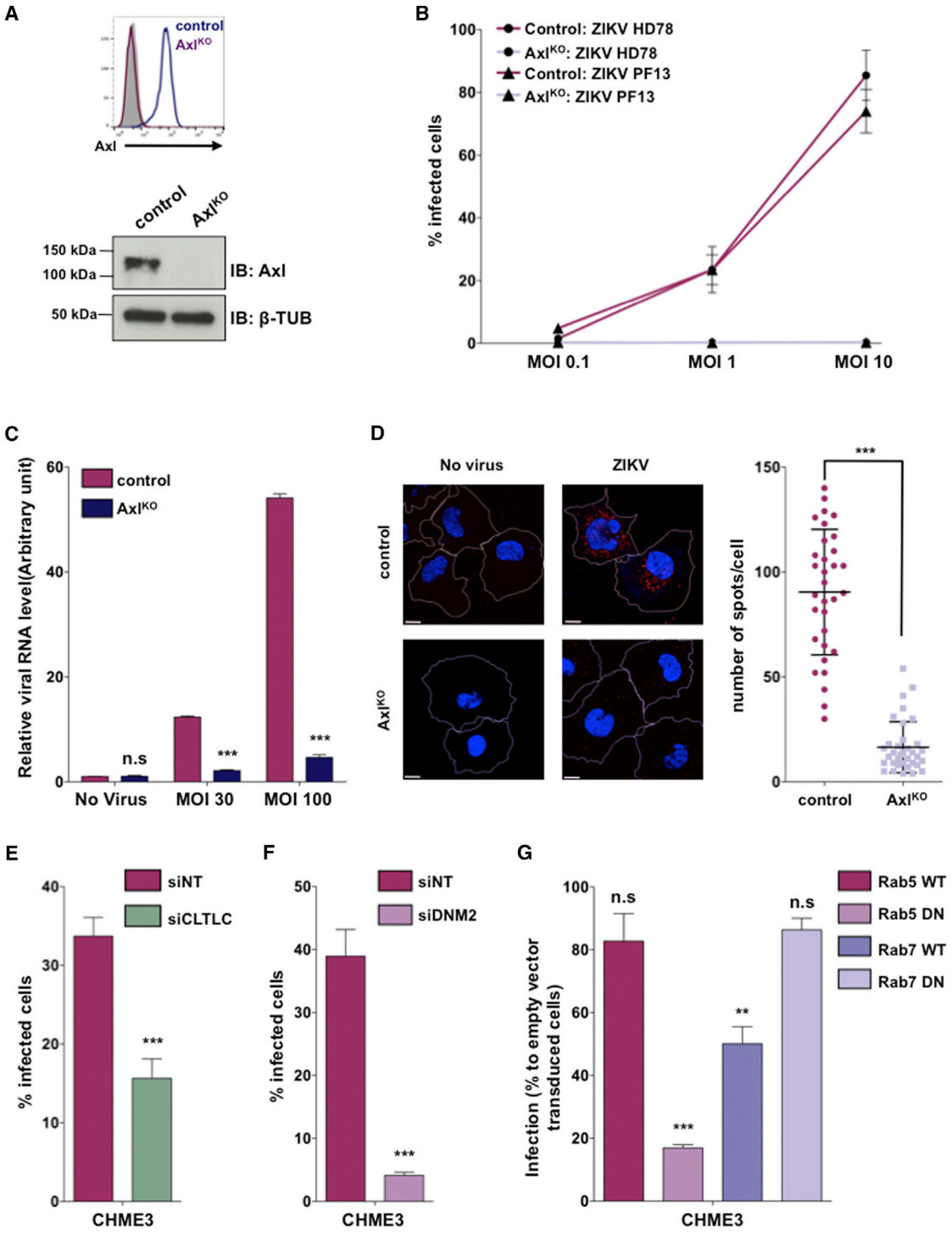

Figure 3. Axl Mediates ZIKV Entry by Clathrin-Mediated Endocytosis and Delivery to Early Endosomes

(A) Validation by flow cytometry and immunoblotting of Axl ablation by CRISPR-Cas9.

(B) CHME3 Axl^{KO} and parental cells were infected with ZIKVHD78 and ZIKV-PF13 at the indicated MOI.

(C) CHME3 Axl^{KO} and parental cells were challenged with ZIKV, total cellular RNA was extracted 4 hpi, and relative viral RNA levels were determined by real-time quantitative PCR. Data shown are means ± SD and are representative of two independent experiments.

(D) CHME cells were incubated on ice with ZIKVHD78 at a MOI of 100 in the presence of rGas6 (5 mM). Cells were shifted at 37°C for 90 min and then fixed, permeabilized, and stained for ZIKV viral RNA (red). White lines outline the cell membranes stained with wheat germ agglutinin, A488-conjugated. The data shown at the left are representative of two independent experiments. Right: quantification of ZIKV RNA spots counted per cell ($n \geq 30$).

(legend continued on next page)

HSV-1 infection was not affected (Figure S3A). ZIKV infection was restored in CHME3 Axl^{KO} cells transduced with an Axl wild-type (WT) cDNA, confirming the importance of Axl in ZIKV infection (Figure S3B). To investigate whether Axl mediates ZIKV endocytosis, we challenged parental and Axl^{KO} CHME3 cells with ZIKVHD78 for 4 hr at 37°C and then treated the cells with trypsin to remove non-internalized viral particles. We next quantified ZIKV RNA levels by real-time qPCR. The amount of internalized viral RNA was significantly reduced in Axl^{KO} cells (Figure 3C). We also performed a fluorescence in situ hybridization (FISH)-based imaging assay (Savidis et al., 2016) to detect viral RNA (vRNA) entry into the cytosol. As shown in Figure 3D, a massive reduction of vRNA was observed 90 min post-infection in Axl^{KO} cells compared with parental cells. Together, these data show that Axl is an essential ZIKV cellular factor that promotes virus entry.

Axl is known to mediate phagocytosis of apoptotic cells (Lemke and Rothlin, 2008), yet flavivirus entry occurs mainly through clathrin-dependent endocytosis (Fernandez-Garcia et al., 2016; van der Schaar et al., 2008). To characterize the endocytic route used by ZIKV to enter Axl-expressing cells, CHME3 cells were treated with siRNAs directed against the clathrin heavy chain (CLTC), an important component of the clathrin triskelion required for clathrin-coated vesicle (CCV) formation (McMahon and Boucrot, 2011). We also silenced Dynamin-2 (DNM2), a GTPase involved in pinching off endocytic vesicles from the plasma membrane (Ferguson and De Camilli, 2012). Forty-eight hours post-transfection, CLTC and DNM2 depletion was assessed by immunoblotting (Figure S3C). Surface expression of Axl was not modified after silencing of clathrin heavy chain (CTLTC) or DNM2 (Figure S3D), but ZIKV infection was strongly impaired in these cells (Figures 3E and 3F). We obtained similar results in HeLa-Axl cells (Figure S3E).

To investigate whether ZIKV fuses within the early or late endosomes, we transduced CHME3 cells with retroviral vectors expressing either the GFP-tagged WT or dominant-negative (DN) forms of Rab5 (which block CCV transport and fusion to early endosomes) or Rab7 (which inhibits cargo delivery to late endosomes) (Fernandez-Garcia et al., 2016). Expression of Rab5DN reduced ZIKV infection by 85% compared with cells transduced with the empty vector (Figure 3G; Figure S3F). Of note, Rab7DN did not inhibit ZIKV infection, whereas Rab7 WT inhibited infection by 50%. Altogether, these results suggest that ZIKV particles are internalized by clathrin and dynamin-dependent endocytosis and delivered to early endosomes, where the mild acidic milieu is optimal to trigger the conformational change of the envelope.

ZIKV Activates Axl Kinase Activity to Antagonize Type I Interferon Signaling

To determine whether Axl kinase activity enhances ZIKV infection, we engineered CHME Axl^{KO} cells stably expressing either WT or a kinase-dead Axl mutant (KM, the K565M mutation lies within the ATP binding site required for kinase activity). These cells expressed similar surface levels of Axl (Figure S4A), and the mutated receptor was catalytically inactive (Figure S4B). Both cells similarly bound ZIKV (data not shown) and mediated vRNA entry into the cytosol with similar efficiency (Figure 4A). ZIKV infection was restored in cells expressing Axl WT (Figure 4B; Figure S4C) and reduced in cells complemented with Axl KM (Figure 4B; Figure S4C). These data indicate that the kinase activity of Axl is important for ZIKV infection and suggest that Axl ligation by ZIKV may initiate signal transduction events that facilitate a post-entry step in the viral life cycle. To directly assess this hypothesis, we analyzed the Axl phosphorylation status in CHME3 cells challenged with ZIKVHD78 in the absence or presence of purified Gas6. As shown in Figure 4C, addition of Gas6 alone led to a dose-dependent activation of Axl, whereas ZIKV bound to Gas6 potentiated Axl phosphorylation (Figure 4C). Consistent with this, we found that R428, a small-molecule inhibitor of Axl kinase activity (Holland et al., 2010; Figure 4D), inhibited ZIKV infection of glial cells in a dose-dependent manner (Figure 4E; Figure S4E) but had no effect on HSV-1 (Figure S4D). Of note, R428 treatment did not block ZIKV entry (Figure 4F; Figure S4F) or affect Axl surface levels (Figure 4F) but significantly reduced viral RNA amplification at a later time point (Figure 4F). Nonetheless, despite statistically robust analysis indicating that differences in vRNA level expression at 4 hours post infection (hpi) were non-significant, we could not rule out that the Axl kinase domain might be partially involved in Axl-mediated ZIKV internalization.

Signaling through Axl dampens the innate immune responses (Rothlin et al., 2007). A recent publication showed that Gas6-coated viruses activate Axl, dampen type I IFN signaling, and promote infection of murine dendritic cells (Bhattacharyya et al., 2013). To evaluate whether Axl kinase activity modulates IFN response to ZIKV, we quantified the levels of IFN-β and SOCS-1 mRNA by qPCR in CHME cells treated with the Axl antagonist R428 and infected by ZIKV. 24 hpi, R428 led to a 4- and 16-fold increase in IFN-β and SOCS1 mRNA levels, respectively (Figure 4G) but also IFNλ1, IFNλ2, and ISG20 (Figure S4G) as well as the pro-inflammatory cytokines tumor necrosis factor α (TNF-α), interleukin-6 (IL-6), or IL-1β (Figure S4H). Of note, IFNβ, SOCS1, and pro-inflammatory cytokine RNA levels were significantly higher in infected CHME Axl^{KO} cells expressing Axl KM compared with Axl WT (Figure 4H; Figure S4I). Overall, these data strongly suggest that ZIKV-mediated activation of Axl may enhance viral replication by mediating a global suppression of innate immunity in glial cells.

In conclusion, we describe a major role of the TAM receptor Axl and its ligand Gas6 in ZIKV infection of glial cells: astrocytes and microglia. Our results complement two recent studies in mouse models (Li et al., 2016b) and in human fetus brain tissue

(E and F) CHME3 cells were transfected with a siRNA pool targeting clathrin heavy chain (siCLTC), Dynamin2 (siDNM2), or a non-targeting siRNA (siNT) as a negative control, and cells were infected with ZIKV.

(G) CHME3 cells were transduced with a retroviral vector expressing the WT or DN forms of EGFP-Rab5 and -Rab7. Cells were challenged 24 hr post-transduction with ZIKV (MOI 5). For each sample, the percentage of infected cells was quantified in the EGFP-positive population. Infection was assessed 24 hpi by flow cytometry. The data shown are means ± SD of two independent experiments. Significance was calculated using a two-sample Student's t test (D–F) or one-way ANOVA statistical test (C and G). $^{**}p < 0.001$, $^{***}p < 0.0001$.

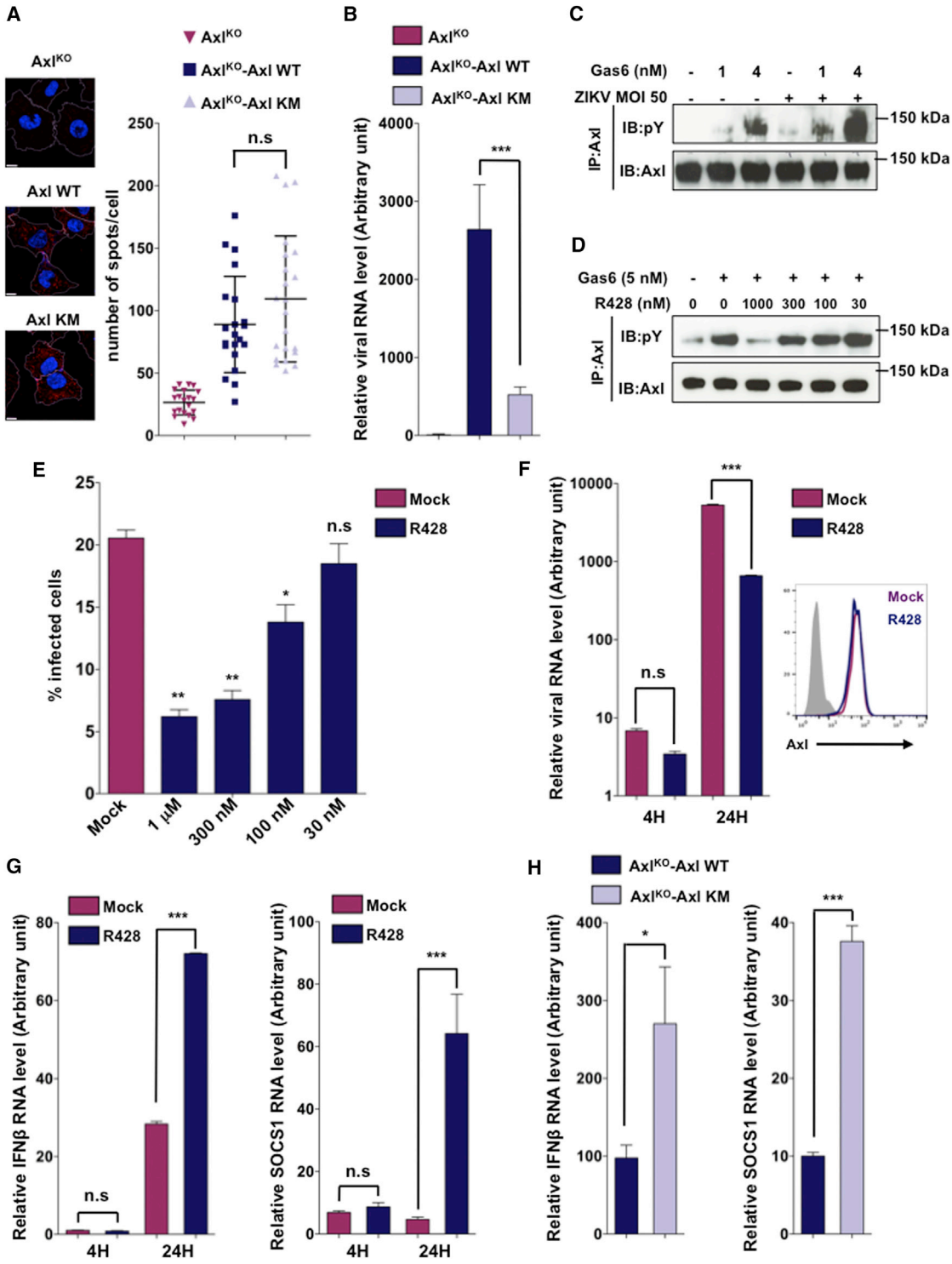

Figure 4. ZIKV Potentiates Axl Kinase Activity to Inhibit the Innate Immunity Response and to Promote Infection

(A) CHME Axl^{KO} cells complemented with a plasmid encoding either a WT Axl or a KM Axl receptor were incubated on ice with ZIKV in the presence of rGas6 (5 mM). Cells were shifted at 37°C for 90 min and then fixed, permeabilized, and stained for ZIKV viral RNA (red) as described in Figure 3. The data shown at the left are representative of two independent experiments. Right: quantification of ZIKV RNA spots counted per cell ($n \geq 20$).

(B) CHME Axl^{KO} cells complemented with Axl WT or Axl KM were challenged with ZIKV (MOI 20). Total cellular RNA was extracted 18 hpi, and relative viral RNA levels were determined by real-time quantitative PCR.

(legend continued on next page)

organotypic cultures (Retallack et al., 2016), showing that astrocytes and microglia support ZIKV infection. We highlight a dual function of Axl/Gas6 during ZIKV infection in brain cells: Axl indirectly binds ZIKV through Gas6 bridging and mediates ZIKV endocytosis through the CME pathway, and Axl is a signaling molecule that is activated by ZIKV-Gas6 complexes during viral entry to dampen innate immunity.

Our data are consistent with the detection of ZIKV antigen in glial cells from brain autopsies of fetuses diagnosed with microcephaly (Martines et al., 2016) and suggest that astrocytes and microglial cell are important ZIKV target cells. Many astrocytes are located in the vicinity of capillaries and could represent one of the first target cells encountered by ZIKV after crossing the blood-brain barrier. Furthermore, astrocytes contributes to BBB maintenance; therefore, their infection by ZIKV may induce BBB leakage, as recently reported in mice (Shao et al., 2016). In addition to being productively infected and potentially serving as a viral reservoir in the CNS, astrocytes and microglial cells could contribute to ZIKV-induced neuro-inflammation by releasing pro-inflammatory cytokines (Osso and Chan, 2015) that might be detrimental to neural stem cell proliferation and differentiation (Ji et al., 2015). This is consistent with a recent study in a mouse model reporting increased expression of cytokines in the developing brain correlating with ZIKV pathogenesis (Li et al., 2016a). In mice and monkeys, microglia have been shown to be activated a few days after ZIKV infection (Huang et al., 2016; Shao et al., 2016). Because microglia activation by LPS reduces precursor cell numbers (Cunningham et al., 2013), it will be worth evaluating how ZIKV infection may contribute to microglia activation and subsequent pathogenesis.

We further report that blocking Axl does not prevent ZIKV infection of hNPCs, suggesting that the virus may use different receptors or pathways depending on the cell type. These data may explain prior findings that Axl-KO mice deficient in type-I IFN signaling remain susceptible to ZIKV (Miner et al., 2016b), probably because of decreased blood-brain barrier integrity or dampened host response (Miner et al., 2015; Schmid et al., 2016). Because our data and previous studies (Bhattacharyya et al., 2013; Rothlin et al., 2007) reveal that one major function of Axl is to modulate innate immunity, it will be of interest to reconsider the implication of Axl during ZIKV infection of type I IFN-competent animals. Interestingly, we show that Axl mediates infection of murine astrocytes, opening the way to explore the role of astrocytes using mouse models of in utero infection (Li et al., 2016a; Wu et al., 2016).

Finally, we identified two antagonists of the Axl/Gas6 pathway (MYD1 and R428) displaying antiviral activity. MYD1 blocks ZIKV binding to Axl by trapping Gas6 and abrogating Axl signaling, whereas the kinase inhibitor R428 blocks Axl phosphorylation and enhances innate immune signaling upon infection. Our results suggest that inhibition of Axl function might protect microglia and astrocytes from infection and may reduce the viral load in the CNS. On a cautious note, interfering with Axl kinase activity could have an adverse effect on neurogenesis by increasing the release of pro-inflammatory cytokines, which may reduce neuronal stem cell proliferation and differentiation (Ji et al., 2013). Furthermore, as reported in mice (Miner et al., 2015; Schmid et al., 2016), global knockdown of Axl may potentiate infection of other Axl-independent cell types (e.g., radial glial cells) by down-modulating immune control of viral spread or facilitating BBB crossing. In this context, it will be of interest to determine, in murine or primate models (Adams Waldorf et al., 2016; Osuna et al., 2016), whether short-term pharmacological inhibition of the Axl/Gas6 pathway, combined with recently identified small-molecule inhibitors of ZIKV infection or induced neural cell death (Xu et al., 2016), could be used for treatment or prophylaxis of ZIKV infection.

EXPERIMENTAL PROCEDURES

Human Tissue Procurement and Processing, Primary Cells, and Human Neural Progenitor Cells

Human fetuses aged 20 and 26 GWs or post-ovulatory week without any neuropathological alterations were collected within 24 hr after legal abortion or spontaneous death. All procedures were approved by the ethics committee (Agence de Biomédicine, approval number PFS12-0011). Tissues were immersion-fixed in 4% paraformaldehyde for 24 hr, cryoprotected in 20% sucrose, and stored at −80°C until use. Tissues were cut into 12-μm-thick coronal sections, mounted on Superfrost slides, and stored at −80°C. Human primary astrocytes were purchased from Lonza and cultured according to the manufacturer's instructions. hNPCs used in this study were prepared as described previously (Brnic et al., 2012).

Ethics Statement

Human fetuses were obtained after legal abortion with written informed consent of the patient. The procedure for the procurement and use of human fetal CNS tissue was approved and monitored by the Comité Consultatif de Protection des Personnes dans la Recherche Biomédicale of Henri Mondor Hospital.

Virus Preparation and Titration

The ZIKV HD78788 strain (obtained via Phillipe Despres, Institut Pasteur) was isolated from a human case in Senegal (1991) (Faye et al., 2014). The ZIKV PF-25013-18 strains (obtained via V. M. Cao-Lormeau Institut Louis Malardé) was

(C) Serum-starved CHME3 cells were incubated for 10 min with increasing concentrations of rGas6 alone or along with ZIKV (MOI 50). Phosphorylation of immunoprecipitated Axl was monitored with a phosphotyrosine-specific antibody (immunoblot: anti-phosphotyrosine [IB: pY]).
(D) CHME3 cells were preincubated for 30 min with or without R428 prior to Gas6 stimulation.
(E) CHME3 cells were preincubated for 30 min with the indicated concentration of R428 or DMSO (mock) and challenged with ZIKV (MOI 2).
(F and G) CHME3 cells were preincubated for 30 min with R428 (1 μM) or DMSO (mock), and cells were challenged with ZIKV (MOI 30) in the continuous presence of the drug. 4 hpi, the virus was washed out. The inset displays cell surface expression of Axl at the time of infection. Total cellular RNA was extracted 4 and 24 hpi, and relative viral RNA levels and IFNβ or SOCS1 mRNA levels were determined by real-time quantitative PCR.
(H) CHME Axl^{KO} cells complemented with Axl WT or Axl KM were challenged with ZIKV (MOI 20). Total cellular RNA was extracted 18 hpi, and IFNβ and SOCS1 mRNA levels were determined by real-time quantitative PCR. Infection was assessed 24 hpi by flow cytometry.
(B and E–H) The data shown are means ± SD and are representative of three independent experiments performed in duplicate.
(A, C, and D) The data shown are representative images of two independent experiments. Significance was calculated using a one-way ANOVA statistical test with a Dunnett's multiple comparisons test (E) or a two-sample Student's t test (A, B, and F–H). *$p < 0.05$, **$p < 0.001$, ***$p < 0.0001$.

isolated from a viremic patient in French Polynesia in 2013 (Cao-Lormeau et al., 2014). Viruses were prepared and titered as described previously (Meertens et al., 2012).

Axl Ablation by CRISPR-Cas9 and Axl Complementation

CHME3 cells were transfected with the lentiCRISPRV2 plasmid encoding the codon-optimized Cas9 nuclease (Addgene) and Axl-specific guide RNA (GGGGACTCACGGGCACCCTTCGG). Transfected cells were selected by puromycin treatment (1 μg/ml) and sorted by fluorescence-activated cell sorting (FACS) for loss of Axl expression after staining with anti-Axl Ab.

Statistical Analyses

Graphical representation and statistical analyses were performed using Prism5 software (GraphPad). Unless otherwise stated, results are shown as means ± SD from three independent experiments. Differences were tested for statistical significance using unpaired two-tailed t test or one-way ANOVA with Tukey post test.

SUPPLEMENTAL INFORMATION

Supplemental Information includes Supplemental Experimental Procedures and four figures and can be found with this article online at http://dx.doi.org/10.1016/j.celrep.2016.12.045.

AUTHOR CONTRIBUTIONS

Conceptualization, L.M., N.J., P.G., and A.A.; Investigation, L.M., A.L., O.D., S.C., L.S., L.B.M., T.L.C., and M.L.H.; Writing – Original Draft, L.M., O.S., and A.A.; Writing – Review & Editing, L.M., S.C., A.Z., M.C., N.J., P.G., O.S., and A.A.; Visualization, L.M. and A.A., Resources, M.C.L., M.C., D.M., R.T., and P.G.; Funding Acquisition, A.A.

ACKNOWLEDGMENTS

This works was supported by NIH Grant R01 AI101400), the European Union Horizon 2020 Research and Innovation Programme under ZIKAlliance Grant Agreement 734548, Labex Integrative Biology of Emerging Infectious Diseases, and the French National Research Agency "Investissements d'Avenir" Program ANR-10-IHUB-0002 and CE14-0029 Grant TIMTAMDEN]. The authors thank Greg Lemke and Erin Lew (Salk Institute) for providing the purified recombinant Gas6. We are most grateful to Dr. C. Montero-Menei for providing hNPCs. We thank Stéphane Dallongeville (Institut Pasteur) for the help with ICY image analysis.

Received: July 8, 2016
Revised: November 28, 2016
Accepted: December 14, 2016
Published: January 10, 2017

REFERENCES

Adams Waldorf, K.M., Stencel-Baerenwald, J.E., Kapur, R.P., Studholme, C., Boldenow, E., Vornhagen, J., Baldessari, A., Dighe, M.K., Thiel, J., Merillat, S., et al. (2016). Fetal brain lesions after subcutaneous inoculation of Zika virus in a pregnant nonhuman primate. Nat. Med. *22*, 1256–1259.

Amara, A., and Mercer, J. (2015). Viral apoptotic mimicry. Nat. Rev. Microbiol. *13*, 461–469.

Bhattacharyya, S., Zagórska, A., Lew, E.D., Shrestha, B., Rothlin, C.V., Naughton, J., Diamond, M.S., Lemke, G., and Young, J.A. (2013). Enveloped viruses disable innate immune responses in dendritic cells by direct activation of TAM receptors. Cell Host Microbe *14*, 136–147.

Brasil, P., Pereira, J.P., Jr., Raja Gabaglia, C., Damasceno, L., Wakimoto, M., Ribeiro Nogueira, R.M., Carvalho de Sequeira, P., Machado Siqueira, A., Abreu de Carvalho, L.M., Cotrim da Cunha, D., et al. (2016). Zika Virus Infection in Pregnant Women in Rio de Janeiro - Preliminary Report. N. Engl. J. Med. *375*, 2321–2334.

Brnic, D., Stevanovic, V., Cochet, M., Agier, C., Richardson, J., Montero-Menei, C.N., Milhavet, O., Eloit, M., and Coulpier, M. (2012). Borna disease virus infects human neural progenitor cells and impairs neurogenesis. J. Virol. *86*, 2512–2522.

Calvet, G., Aguiar, R.S., Melo, A.S., Sampaio, S.A., de Filippis, I., Fabri, A., Araujo, E.S., de Sequeira, P.C., de Mendonça, M.C., de Oliveira, L., et al. (2016). Detection and sequencing of Zika virus from amniotic fluid of fetuses with microcephaly in Brazil: a case study. Lancet Infect. Dis. *16*, 653–660.

Cao-Lormeau, V.M., Roche, C., Teissier, A., Robin, E., Berry, A.L., Mallet, H.P., Sall, A.A., and Musso, D. (2014). Zika virus, French polynesia, South pacific, 2013. Emerg. Infect. Dis. *20*, 1085–1086.

Carod-Artal, F.J., Wichmann, O., Farrar, J., and Gascón, J. (2013). Neurological complications of dengue virus infection. Lancet Neurol. *12*, 906–919.

Cunningham, C.L., Martínez-Cerdeño, V., and Noctor, S.C. (2013). Microglia regulate the number of neural precursor cells in the developing cerebral cortex. J. Neurosci. *33*, 4216–4233.

Dick, G.W., Kitchen, S.F., and Haddow, A.J. (1952). Zika virus. I. Isolations and serological specificity. Trans. R. Soc. Trop. Med. Hyg. *46*, 509–520.

Faye, O., Freire, C.C., Iamarino, A., Faye, O., de Oliveira, J.V., Diallo, M., Zanotto, P.M., and Sall, A.A. (2014). Molecular evolution of Zika virus during its emergence in the 20(th) century. PLoS Negl. Trop. Dis. *8*, e2636.

Ferguson, S.M., and De Camilli, P. (2012). Dynamin, a membrane-remodelling GTPase. Nat. Rev. Mol. Cell Biol. *13*, 75–88.

Fernández-Fernández, L., Bellido-Martín, L., and García de Frutos, P. (2008). Growth arrest-specific gene 6 (GAS6). An outline of its role in haemostasis and inflammation. Thromb. Haemost. *100*, 604–610.

Fernandez-Garcia, M.D., Meertens, L., Chazal, M., Hafirassou, M.L., Dejarnac, O., Zamborlini, A., Despres, P., Sauvonnet, N., Arenzana-Seisdedos, F., Jouvenet, N., and Amara, A. (2016). Vaccine and Wild-Type Strains of Yellow Fever Virus Engage Distinct Entry Mechanisms and Differentially Stimulate Antiviral Immune Responses. MBio *7*, e01956–e15.

Fourgeaud, L., Través, P.G., Tufail, Y., Leal-Bailey, H., Lew, E.D., Burrola, P.G., Callaway, P., Zagórska, A., Rothlin, C.V., Nimmerjahn, A., and Lemke, G. (2016). TAM receptors regulate multiple features of microglial physiology. Nature *532*, 240–244.

Hamel, R., Dejarnac, O., Wichit, S., Ekchariyawat, P., Neyret, A., Luplertlop, N., Perera-Lecoin, M., Surasombatpattana, P., Talignani, L., Thomas, F., et al. (2015). Biology of Zika Virus Infection in Human Skin Cells. J. Virol. *89*, 8880–8896.

Holland, S.J., Pan, A., Franci, C., Hu, Y., Chang, B., Li, W., Duan, M., Torneros, A., Yu, J., Heckrodt, T.J., et al. (2010). R428, a selective small molecule inhibitor of Axl kinase, blocks tumor spread and prolongs survival in models of metastatic breast cancer. Cancer Res. *70*, 1544–1554.

Huang, W.C., Abraham, R., Shim, B.S., Choe, H., and Page, D.T. (2016). Zika virus infection during the period of maximal brain growth causes microcephaly and corticospinal neuron apoptosis in wild type mice. Sci. Rep. *6*, 34793.

Ji, R., Tian, S., Lu, H.J., Lu, Q., Zheng, Y., Wang, X., Ding, J., Li, Q., and Lu, Q. (2013). TAM receptors affect adult brain neurogenesis by negative regulation of microglial cell activation. J. Immunol. *191*, 6165–6177.

Ji, R., Meng, L., Li, Q., and Lu, Q. (2015). TAM receptor deficiency affects adult hippocampal neurogenesis. Metab. Brain Dis. *30*, 633–644.

Kariolis, M.S., Miao, Y.R., Jones, D.S., 2nd, Kapur, S., Mathews, I.I., Giaccia, A.J., and Cochran, J.R. (2014). An engineered Axl 'decoy receptor' effectively silences the Gas6-Axl signaling axis. Nat. Chem. Biol. *10*, 977–983.

Lemke, G., and Rothlin, C.V. (2008). Immunobiology of the TAM receptors. Nat. Rev. Immunol. *8*, 327–336.

Li, C., Xu, D., Ye, Q., Hong, S., Jiang, Y., Liu, X., Zhang, N., Shi, L., Qin, C.F., and Xu, Z. (2016a). Zika Virus Disrupts Neural Progenitor Development and Leads to Microcephaly in Mice. Cell Stem Cell *19*, 672.

Li, H., Saucedo-Cuevas, L., Regla-Nava, J.A., Chai, G., Sheets, N., Tang, W., Terskikh, A.V., Shresta, S., and Gleeson, J.G. (2016b). Zika Virus Infects Neural Progenitors in the Adult Mouse Brain and Alters Proliferation. Cell Stem Cell *19*, 593–598.

Martines, R.B., Bhatnagar, J., de Oliveira Ramos, A.M., Davi, H.P., Iglezias, S.D., Kanamura, C.T., Keating, M.K., Hale, G., Silva-Flannery, L., Muehlenbachs, A., et al. (2016). Pathology of congenital Zika syndrome in Brazil: a case series. Lancet *388*, 898–904.

McMahon, H.T., and Boucrot, E. (2011). Molecular mechanism and physiological functions of clathrin-mediated endocytosis. Nat. Rev. Mol. Cell Biol. *12*, 517–533.

Meertens, L., Carnec, X., Lecoin, M.P., Ramdasi, R., Guivel-Benhassine, F., Lew, E., Lemke, G., Schwartz, O., and Amara, A. (2012). The TIM and TAM families of phosphatidylserine receptors mediate dengue virus entry. Cell Host Microbe *12*, 544–557.

Miner, J.J., Daniels, B.P., Shrestha, B., Proenca-Modena, J.L., Lew, E.D., Lazear, H.M., Gorman, M.J., Lemke, G., Klein, R.S., and Diamond, M.S. (2015). The TAM receptor Mertk protects against neuroinvasive viral infection by maintaining blood-brain barrier integrity. Nat. Med. *21*, 1464–1472.

Miner, J.J., Cao, B., Govero, J., Smith, A.M., Fernandez, E., Cabrera, O.H., Garber, C., Noll, M., Klein, R.S., Noguchi, K.K., et al. (2016a). Zika Virus Infection during Pregnancy in Mice Causes Placental Damage and Fetal Demise. Cell *165*, 1081–1091.

Miner, J.J., Sene, A., Richner, J.M., Smith, A.M., Santeford, A., Ban, N., Weger-Lucarelli, J., Manzella, F., Rückert, C., Govero, J., et al. (2016b). Zika Virus Infection in Mice Causes Panuveitis with Shedding of Virus in Tears. Cell Rep. *16*, 3208–3218.

Mlakar, J., Korva, M., Tul, N., Popović, M., Poljšak-Prijatelj, M., Mraz, J., Kolenc, M., Resman Rus, K., Vesnaver Vipotnik, T., Fabjan Vodušek, V., et al. (2016). Zika Virus Associated with Microcephaly. N. Engl. J. Med. *374*, 951–958.

Nowakowski, T.J., Pollen, A.A., Di Lullo, E., Sandoval-Espinosa, C., Bershteyn, M., and Kriegstein, A.R. (2016). Expression Analysis Highlights AXL as a Candidate Zika Virus Entry Receptor in Neural Stem Cells. Cell Stem Cell *18*, 591–596.

Osso, L.A., and Chan, J.R. (2015). Astrocytes Underlie Neuroinflammatory Memory Impairment. Cell *163*, 1574–1576.

Osuna, C.E., Lim, S.Y., Deleage, C., Griffin, B.D., Stein, D., Schroeder, L.T., Omange, R., Best, K., Luo, M., Hraber, P.T., et al. (2016). Zika viral dynamics and shedding in rhesus and cynomolgus macaques. Nat. Med. *22*, 1448–1455.

Retallack, H., Di Lullo, E., Arias, C., Knopp, K.A., Sandoval-Espinosa, C., Laurie, M.T., Zhou, Y., Gormley, M., Mancia Leon, W.R., Krencik, R., et al. (2016). Zika Virus in the Human Placenta and Developing Brain: Cell Tropism and Drug Inhibition. bioRxiv, Published online June 15, 2016. 10.1101/058883.

Rothlin, C.V., Ghosh, S., Zuniga, E.I., Oldstone, M.B., and Lemke, G. (2007). TAM receptors are pleiotropic inhibitors of the innate immune response. Cell *131*, 1124–1136.

Savidis, G., Perreira, J.M., Portmann, J.M., Meraner, P., Guo, Z., Green, S., and Brass, A.L. (2016). The IFITMs Inhibit Zika Virus Replication. Cell Rep. *15*, 2323–2330.

Schmid, E.T., Pang, I.K., Carrera Silva, E.A., Bosurgi, L., Miner, J.J., Diamond, M.S., Iwasaki, A., and Rothlin, C.V. (2016). AXL receptor tyrosine kinase is required for T cell priming and antiviral immunity. eLife *5*, e12414.

Shao, Q., Herrlinger, S., Yang, S.L., Lai, F., Moore, J.M., Brindley, M.A., and Chen, J.F. (2016). Zika virus infection disrupts neurovascular development and results in postnatal microcephaly with brain damage. Development *143*, 4127–4136.

Tang, H., Hammack, C., Ogden, S.C., Wen, Z., Qian, X., Li, Y., Yao, B., Shin, J., Zhang, F., Lee, E.M., et al. (2016). Zika Virus Infects Human Cortical Neural Progenitors and Attenuates Their Growth. Cell Stem Cell *18*, 587–590.

van der Schaar, H.M., Rust, M.J., Chen, C., van der Ende-Metselaar, H., Wilschut, J., Zhuang, X., and Smit, J.M. (2008). Dissecting the cell entry pathway of dengue virus by single-particle tracking in living cells. PLoS Pathog. *4*, e1000244.

White, M.K., Wollebo, H.S., David Beckham, J., Tyler, K.L., and Khalili, K. (2016). Zika virus: An emergent neuropathological agent. Ann. Neurol. *80*, 479–489.

Wu, K.Y., Zuo, G.L., Li, X.F., Ye, Q., Deng, Y.Q., Huang, X.Y., Cao, W.C., Qin, C.F., and Luo, Z.G. (2016). Vertical transmission of Zika virus targeting the radial glial cells affects cortex development of offspring mice. Cell Res. *26*, 645–654.

Xu, M., Lee, E.M., Wen, Z., Cheng, Y., Huang, W.K., Qian, X., Tcw, J., Kouznetsova, J., Ogden, S.C., Hammack, C., et al. (2016). Identification of small-molecule inhibitors of Zika virus infection and induced neural cell death via a drug repurposing screen. Nat. Med. *22*, 1101–1107.